

Superconductivity on the verge of electronic topological transition in Fe based superconductors

Haranath Ghosh, Smritijit Sen

Indus Synchrotrons Utilization Division, Raja Ramanna Centre for Advanced Technology, Indore -452013, India.
and Homi Bhabha National Institute, Anushakti Nagar, Mumbai 400094, India.

Doping as well as temperature driven Lifshitz transitions are found from first principles simulations in a variety of Fe based superconductors that are consistent with experimental findings. In all the studied compounds the Lifshitz transitions are consistently found to occur at a doping concentration where superconductivity is highest and magnetism disappears. Systematically, the Lifshitz transition occurs in the electron Fermi surfaces for hole doping, whereas in hole Fermi surfaces for electron doping as well as iso-electronic doping. Temperature driven Lifshitz transition is found to occur in the iso-electronic Ru-doped BaFe_2As_2 compounds. Fermi surface areas are found to carry sensitivity of topological modifications more acutely than the band structures and can be used as a better experimental probe to identify electronic topological transition.

Electronic topological transition of the Fermi surface with no broken symmetries, known as Lifshitz transition plays a significant role in numerous branches of condensed matter physics. For example, the collapse of the normal state pseudogap at a Lifshitz transition in $\text{Bi}_2\text{Sr}_2\text{CaCu}_2\text{O}_{8+\delta}$ cuprate superconductor [1], Lifshitz transition in underdoped cuprates [2], Dirac semi metal [3], relativistic insulator NaOsO_3 [4], discontinuous Lifshitz transition in Na_xCoO_2 [5], Zeeman driven Lifshitz transition in YbRh_2Si_2 [6], in two-dimensional Hubbard model [7], bilayer graphene [8], Quantum Hall Liquids [9], to mention a few. Lifshitz transition is recently considered as a quantum phase transition in strongly correlated electron systems also plays a remarkable role in Fe-based high T_c superconductors owing to its special ‘Fermiology’ and multi-band nature [10, 11]. The phase diagrams of Fe-based superconductors (SCs) consist of a number of exhilarating features apart from its novel superconducting phase [12–16]. Various phases are very much sensitive to external parameters like impurity, doping, temperature and pressure. On the other hand, Lifshitz transitions are experimentally observed with respect to some of the above mentioned external parameters [17–19]. Therefore, topological transitions, magnetism and superconductivity which occurs in a variety of materials in condensed matter physics is a subject of general interest.

The Fe-based high T_c SCs being a multiband system has multiple Fermi surfaces (FS) (two electron like and three hole like), any of the FSs may collapse (become smaller ones) either because, some of the bands that crosses the Fermi level (FL) may move away (above or below) from the FL or due to topological modifications (*e.g.*, electron like band transforming to hole like or vice versa) under external perturbation. Lifshitz transition (LT) or electronic topological transition (ETT), where FSs/electronic bands alter topology, have been usually investigated as zero temperature phenomena arising due to impurity, doping or pressure etc. However, temperature dependent LT/ETT is observed recently in WTe_2 [20]. The consequences of these LT/ETT are innumerable. It can lead to reduced interband scattering (af-

fecting mechanism of SC), nesting of FS (affecting magnetism), anomalies or singularities in the density of states at FL and in general anomalies in the kinematics, dynamics and thermodynamics of electrons, which would affect various physical properties [21]. LT/ETT are also observed in Fe-based SCs induced by pressure, impurity and doping [11, 17, 22–24]. In particular, for BaFe_2As_2 (Ba122) system, LT is predicted theoretically due to small but unintentional Sn impurity in contrast to other compounds like SrFe_2As_2 (Sr122) and CaFe_2As_2 (Ca122) [23]. In hole doped Ba122, LT is found in the heavily doped regime as evident from the theoretical work of Khan *et al.*, [11]. On the other hand, LT in electron (Co in place of Fe) doped Ba122 is observed experimentally [20]. But the temperature induced LT in general is rare; we have predicted temperature dependent LT in Ru doped Ba122 system. In this letter, we show with explicit demonstrations in a series of Fe-based SCs that the LT / ETT occur at a doping concentration where SC is maximum and magnetism/structural transition vanishes.

Determining LT/ETT experimentally is challenging specially in systems that constitute multi-orbital-derived FS like Fe-based SCs; we show that the FS area (FSA) carries sensitivity of topological modifications more acutely than the band structures (BS) and this can be used as a better experimental tool to identify ETT/LT. As a result of LT or ETT the FSA of a particular FS gets largely affected and hence a systematic study of FSA as a function of doping is most desirable. A detailed study on the variations of FSA, *e.g.*, variations of (i) areas of each individual FSs, (ii) sum total areas of all the electron FSs, (iii) sum total areas of all the hole FSs, (iv) sum total areas of all the five FSs, (v) difference of all hole and all electron FS areas as a function of doping is a rare wealth of information that can be verified by the de Haas-van Alphen and allied effects (*i.e.*, Shubnikov-de Haas effect) are presented in this letter. All the above FS areas with doping show distinctly different behaviors below and above the ETT. Clear deviation in the variations of FSA with doping marks the occurrence of topological transition (TT). This can therefore lead

to a step forward progress in the experimental detection of LT/ETT in general. It is worthwhile mentioning here that in the overdoped regime of high- T_c cuprate SCs, ARPES and quantum oscillation studies revealed large FS but not only its shape and size change with doping but also breaks up into Fermi arcs [25] which turned out to be closed hole Fermi pocket [26–29]. All these points to a question, are high T_c SCs topological or whether the high T_c is restricted by TT ?!

First principles density functional theories (DFT) can produce correct solutions of the many electron Schrödinger equation if exact electronic density is used as input. Various modern X-ray diffraction techniques *e.g.*, using Synchrotrons radiation source etc. that determines crystallographic information at different external perturbations are essentially result of diffraction from various atomic charge densities (Bragg's diffraction). Considering experimentally determined structural parameters at different temperatures (doping) as input thus in turn provides temperature (doping) dependent exact densities in our first principles calculation. These input structural parameters are kept fixed through out the calculation for a fixed temperature (doping). The main effect on the electronic structure from finite temperature is the underlying crystal structure, and the average crystal structure at finite temperature can usually be reliably determined from diffraction experiment at a given temperature. Our first principles calculations are performed by implementing ultrasoft pseudopotential with plane wave basis set based on DFT [30]. Electronic exchange correlation is treated within the generalised gradient approximation (GGA) using Perdew-Burke-Ernzerhof (PBE) functional [31]. Electronic structures (BS, FS *etc.*), calculated using optimized lattice parameters (a , b , c and z_{As}) do not resemble with that of the experimentally measured one [32, 33]. This insist us to employ experimental lattice parameters *i.e.*, a , b , c and z_{As} [13, 14, 34, 36, 37] as a function of doping and temperature both in the low temperature orthorhombic as well as in the high temperature tetragonal phases as inputs of our first principles calculations. In order to dope, we use Virtual crystal approximation (VCA) [38]. Non-spin-polarized and spin polarised single point energy calculations are performed for tetragonal phase with space group symmetry I4/mmm (No. 139) and orthorhombic phase with space group symmetry Fmmm (No. 69) respectively with energy cut off 500 eV and higher as well as self-consistent field (SCF) tolerance as 10^{-7} eV/atom. Brillouin zone is sampled in the k-space within MonkhorstPack scheme and grid size for SCF calculation is chosen as per requirement of the calculation for different systems. For simulating FS, grid size of SCF calculation is chosen as $26 \times 26 \times 31$.

We investigate the role of various kinds of dopings (*e.g.*, electron, hole or iso-electronic) in ETT / LT of various Fe-based superconductors $[\text{Ba}_{1-x}\text{M}_x\text{Fe}_2\text{As}_2$ ($\text{M} = \text{K}, \text{Na}$) (see Figs. 1 (a–f)), $\text{BaFe}_{2-x}\text{Co}_x\text{As}_2$ (see Figs. 1 (g–i)), $\text{BaFe}_2\text{As}_{2-x}\text{P}_x$ (see Figs. 1 (j–l))]. In Fig.1(a–c) leftmost pair of columns, we depict the FSs of K doped Ba122 sys-

tems. It is very clear from Fig.1 that there are five Fermi pockets, two around X and Y points (electron like) and three around Γ point (hole like). We find that one of the electron like FSs around X/Y point transform into a different topology (*cf.* right column Fig. 1(c)). We display orbital projected BS of $\text{Ba}_{1-x}\text{K}_x\text{Fe}_2\text{As}_2$ around X point separately in Fig.2(a,b) for $x = 0.2$ and $x = 0.5$ respectively. Same colour codes are used for all orbital resolved BSs throughout. From Fig.2 (a,b) it is quite clear that the electron like nature of d_{xz} band around X (Y) points transform into hole like band; one of the hole like d_{xy} bands also gets modified to an electron like band as a result of K-doping. These topological transformations of FSs/BSs are identified as ETT or LT.

In Fig.1(d – f) we present the FSs of $\text{Ba}_{1-x}\text{Na}_x\text{Fe}_2\text{As}_2$ for various doping concentrations (x). Similar to the ETT found in $\text{Ba}_{1-x}\text{K}_x\text{Fe}_2\text{As}_2$ materials, $\text{Ba}_{1-x}\text{Na}_x\text{Fe}_2\text{As}_2$ also exhibits the same at around the same x . BSs of Na doped Ba122 systems presented in Fig.2 (c,d) are qualitatively very similar to that of the K doped Ba122 system. So we conclude from these two hole doped superconductors that the ETT are found in the electron like bands around the X and Y points at nearly 50% hole doping. Remarkably, the established phase diagrams of the hole doped Ba122 SCs indicate that the highest achievable T_c is also around 50% K (Na) doping where we found LT.

In Fig.1 (g–i), we display FSs of $\text{BaFe}_{2-x}\text{Co}_x\text{As}_2$ (electron doped Fe based SC) in the tetragonal phase. It is quite evident from the right column figures 1 (g–i) that one of the inner hole like FSs around Γ point is modified remarkably due to Co doping. For $x = 0.228$ (*i.e.*, around 11 % of Co doping) in $\text{BaFe}_{2-x}\text{Co}_x\text{As}_2$ system, the FS around Γ point vanishes which corresponds to a topological change in the FS, bears the signature of LT. These findings are quite consistent with experimental observation [10]. In Fig.2 (e–f), we show electronic BS of $\text{BaFe}_{2-x}\text{Co}_x\text{As}_2$. The hole like (d_{xy}) band that lies well above FL for $x = 0.026$ (Fig. 2e) moves below the FL with higher Co doping $x = 0.228$ (Fig. 2f) causing doping induced topological change in the FS. Note $\text{BaFe}_{2-x}\text{Co}_x\text{As}_2$ SCs have maximum T_c at around 11% doping where LT is found from our calculation. Therefore, both the hole doped as well as electron doped systems exhibit LT where SC attains maximum T_c and magnetism vanishes in Fe-based SCs. It should also be noted here that on the contrary to hole doped Ba122 systems, LT in the electron doped Fe-based SCs occurs in the hole FS around Γ point. Our findings are very much consistent with the previous experimental findings [17].

We study the FSs and BSs of $\text{BaFe}_2(\text{As}_{1-x}\text{P}_x)_2$ for various isovalent P dopings in two different structural phases at different temperatures (low temperature orthorhombic phase and high temperature tetragonal phase). It is quite evident from the right column of Figs.1 (j–l) that the topology of one of the hole like FSs is getting modified with increasing P doping. Our calculated orbital resolved BSs shown in Figs.2 (g–l) distinctly reflect sig-

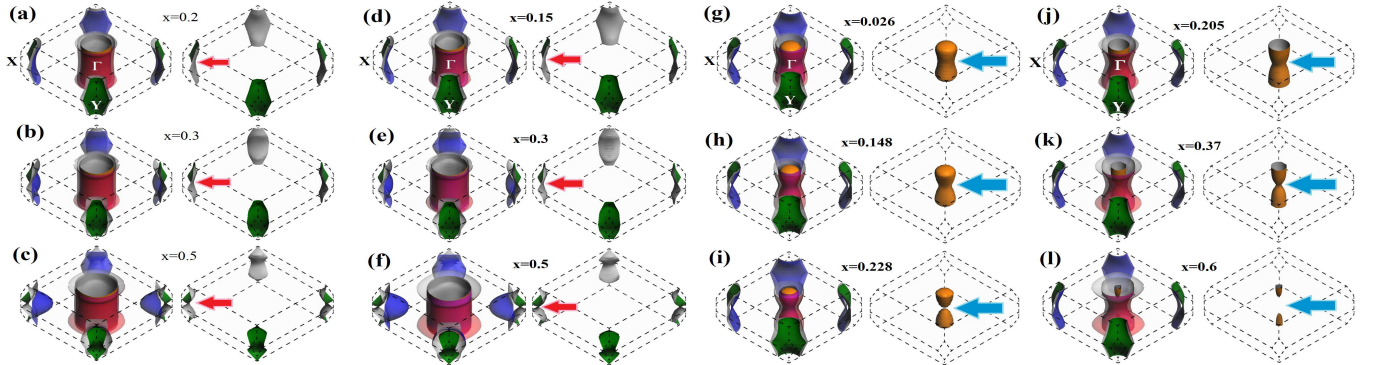


FIG. 1: (Colour online) Calculated FSs in four pair of columns for (i) $\text{Ba}_{1-x}\text{K}_x\text{Fe}_2\text{As}_2$ (a —c); (ii) $\text{Ba}_{1-x}\text{Na}_x\text{Fe}_2\text{As}_2$ (d —f) in the low temperature orthorhombic phase; (iii) $\text{BaFe}_{2-x}\text{Co}_x\text{As}_2$ (g—i) in the high temperature tetragonal phase and (iv) $\text{BaFe}_2(\text{As}_{1-x}\text{P}_x)_2$ (j—l) in the low temperature orthorhombic phase for various dopings as indicated in the figure. In the left columns of each pair, all the five FSs around Γ (hole like), X and Y (electron like) points are shown using different colours for each compounds whereas in the right columns of the same pair, topologically modified FSs are shown separately.

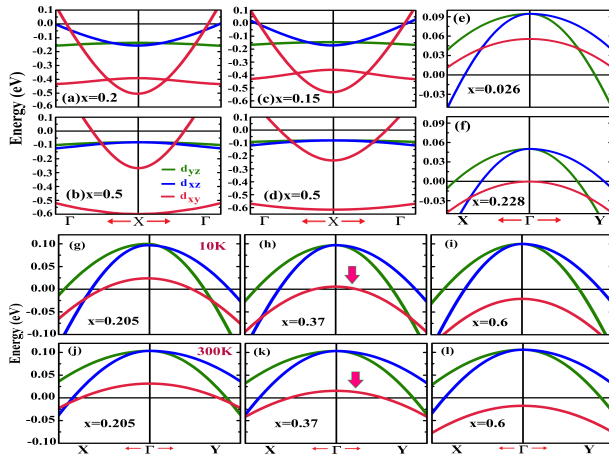


FIG. 2: (Colour online) Zoomed orbital resolved electronic BSs around the high symmetry points where TTs are found in Figs.1 for (i) $\text{Ba}_{1-x}\text{K}_x\text{Fe}_2\text{As}_2$ (a-b); (ii) $\text{Ba}_{1-x}\text{Na}_x\text{Fe}_2\text{As}_2$ (c-d); (iii) $\text{BaFe}_{2-x}\text{Co}_x\text{As}_2$ (e-f) and (iv) $\text{BaFe}_2(\text{As}_{1-x}\text{P}_x)_2$ (g-l). Topological modifications in the d_{xz} , d_{xy} bands from electron to hole like dispersion is observed as doping is increased (cf. (a,b) and (c,d)). LT in the d_{xy} bands of $\text{BaFe}_{2-x}\text{Co}_x\text{As}_2$ [Figs.(e-f)] and $\text{BaFe}_2(\text{As}_{1-x}\text{P}_x)_2$ [Figs.(g-l)] are worth observing.

natures of LT as a result of larger P doping. One of the bands, namely the d_{xy} band around Γ point, well above the FL moves below the FL. We compare the signatures of LT/ETT between two structural phases through orbitally resolved BSs of $\text{BaFe}_2(\text{As}_{1-x}\text{P}_x)_2$ in the low temperature orthorhombic phase (Fig.2(g,h,i)) and the high temperature tetragonal phase (Fig.2 (j, k, l)) for various x . This part of the work thus demonstrates combined doping and temperature induced LT. In both the phases (10K and 300K), d_{xy} band around Γ point goes below FL at $x = 0.6$. But a closer look at the BSs of $\text{BaFe}_2(\text{As}_{1-x}\text{P}_x)_2$ with $x = 0.37$ at 10K and at 300K, re-

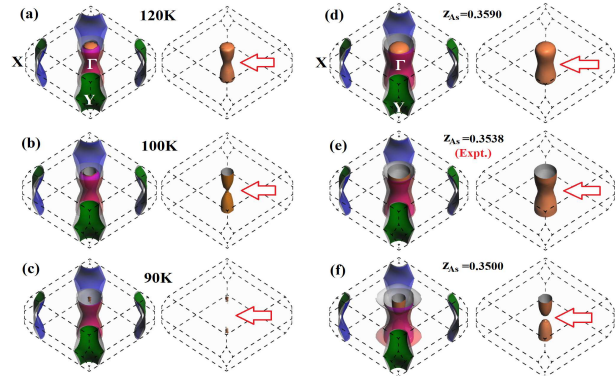


FIG. 3: (Colour online) Calculated FS of $\text{BaFe}_{2-x}\text{Ru}_x\text{As}_2$ below structural transition (pair of left columns) and that of undoped BaFe_2As_2 for different z_{As} (pair of right columns). From each pair of columns, in the left column all the five FSs around Γ (hole like), X and Y (electron like) points are displayed using different colours while in the right column topologically modified inner hole FSs are indicated by arrows.

veal that there are important differences in the BSs. In case of BS of orthorhombic phase (10K) (which is in SC phase), the d_{xy} band is about to cross the FL (Lifshitz point) but on the other hand in case of non-SC tetragonal phase (300K) d_{xy} lies above the FL (FSAs in the two cases are different, see below). This provides an indication of the influence of temperature and structural phase, on ETT/LT. Note in this case also LT occurs at a doping where SC is maximum and no magnetism. From Figs.2(g-l) one can see that the d_{xz} and d_{yz} bands are hardly affected by P doping at As sites, but d_{xy} bands are very sensitive to doping concentration. One of the possible reasons of this fact may arise from the structural modification caused by P doping on As site (Fe-As hybridization modifies anion height characterized by z_{As}). This fact is adequately demonstrated in Fig.4.

In case of $\text{BaFe}_{2-x}\text{Ru}_x\text{As}_2$ also, we find LT (not shown

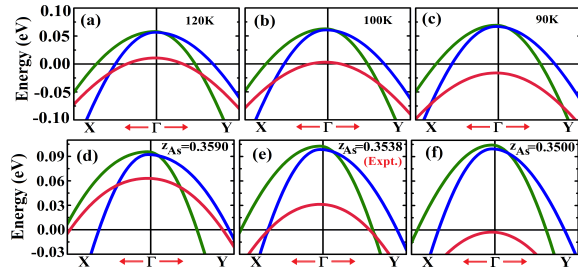


FIG. 4: (Colour online) Calculated orbitally resolved zoomed BSs of $\text{BaFe}_{2-x}\text{Ru}_x\text{As}_2$ in the low temperature orthorhombic phase for three different temperatures (top row). Calculated BSs of BaFe_2As_2 for three different values of z_{As} around Γ point.

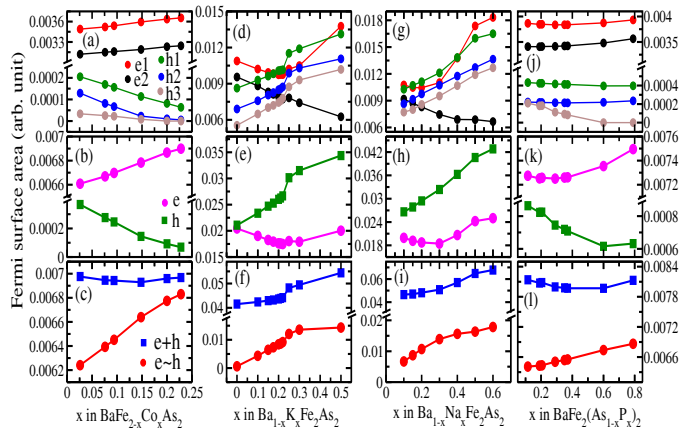


FIG. 5: (Colour online) FSAs of various doped Fe-based SCs namely Co doped (1st column), K doped (2nd column), Na doped (3rd column) and P doped (4th column), as a function of doping concentration. First row, FSA of each individual FSs with doping; sudden change in slopes at the Lifshitz point is worth noting. Second row, total electron and hole FSAs as a function of doping; jumps/change in slopes at the Lifshitz doping is noticeable. Third row, total FSAs and the difference in the FSAs of electron and hole FSs. Remarkable modification of the later at the Lifshitz doping is seen.

here for brevity) at relatively higher Ru doping concentration ($>50\%$) where SC T_c reaches its maximum. This is consistent with the findings of earlier theoretical work on Sr122 system [24]. Below we present the temperature induced LT in 5% Ru doped BaFe_2As_2 . It is well established that the electronic structure of Fe-based SCs is highly sensitive to temperature [34, 35, 40, 41]. It should also be noted that the structural parameters which essentially control the electronic structures of these systems, have significant temperature dependencies [13, 34, 42, 43]. We found temperature dependent LT in 5% Ru doped Ba122 system ($\text{BaFe}_{2-x}\text{Ru}_x\text{As}_2$ with $x = 0.1$) (cf Fig.3) where inner hole FS at 90 K nearly vanishes. In Fig.4, we depict the BSs of $\text{BaFe}_{2-x}\text{Ru}_x\text{As}_2$ ($x = 0.1$) around Γ point which clearly show that the d_{xy} band near FL goes below FL as temperature is lowered

from 120K to 90K. Temperature induced LT is not very common in Fe-based superconductors. To find the root cause of temperature dependent LT, we carry out further calculations on undoped Ba122 [39] with various z_{As} around the experimental value. Essentially we find from Figs.3 (d-f), 4 (d-f) that electronic structures very near to the FL are heavily influenced by z_{As} and it reproduces the overall essential features of temperature induced LT in Ru as well as P doped Ba122 SCs.

FSAs as a function of various kinds of doping shown in Fig.5 can be experimentally measured and turns out to be a unique way of identifying ETT/LT. Normally, hole doping would enlarge (reduce) hole (electron) FSA in contrast to electron doping that would enlarge (reduce) electron (hole) FSA. But in case of any particular FS undergoing TT it would follow against the above and such signatures are remarkably visible in Figs.5(d),(e),(g),(h),(k)). The red curves in Fig.5 (d,g) suggest electron-FSA initially gets reduced with hole doping but increases after certain hole doping because that FS undergoes topological modification from electron like to hole like. This has caused sudden increase in the FSAs of hole-FSs see e.g, green, blue, pink curves of Fig.5 (d,e) around the LT. Thus FSA are found to carry sensitivity of topological modifications more acutely than the BSs and can be used as a better experimental tool to identify ETT/LT. The difference in FSAs of hole and electron FSs indicate net electronic charge density which increases with doping (cf red curves in Fig.5 (c,f,i,l)) as expected, but the slope of the curves are different for different materials. This is consistent with experiments [44]. The doping induced net charge density vary differently below and above the LT, much slowly above the LT indicating less effective doping above LT (cf Fig.5 (i,f,l))); absence of a particular FS due to LT further reduces density of states at FL and thereby high T_c would be limited [45].

We have systematically shown in a variety of high T_c Fe-based SCs that SC occurs at the verge of LT/ETT where magnetism disappears. This is achieved through detailed evaluation of FSs through first principles simulations with experimental structural parameters as a function of doping (temperature) as inputs and detailed demonstrations of LT/ETT. The doping induced net charge density is found to be suppressed at the LT/ETT. This definitely indicates the intriguing need to the inter-relationship between SC and LT in Fe-based SCs. We have also provided a new way of detecting LT/ETT, through evaluation of FSA as a function of doping or temperature as the case may be which can be experimentally performed and is applicable in general to any system. This may modify the experimental phase diagram of Fe-SCs as far as the location of ETT/LT are concerned. We believe our work will open up many theoretical as well as experimental research activities in this direction.

Acknowledgements We thank Dr. P. A. Naik and Dr. P. D. Gupta for their encouragement in this work.

One of us (SS) acknowledges the HBNI, RRCAT for fi-

nancial support and encouragements.

[1] S. Benhabib *et al.*, Phys. Rev. Lett. **114**, 147001 (2015).
 [2] M. R. Norman *et al.*, Phys. Rev. B **81**, 180513(R) (2010).
 [3] Su-Yang Xu *et al.*, Phys. Rev. B **92**, 075115 (2015).
 [4] B. Kim, *et al.*, arXiv:1601.03310 (2016).
 [5] Y. Okamoto, *et al.*, Phys. Rev. B **81**, 121102(R)(2010).
 [6] A. Hackl *et al.*, Phys. Rev. Lett. **106**, 137002 (2011).
 [7] K.-S. Chen, *et al.*, Phys. Rev. B **86**, 165136 (2012).
 [8] Y. Lemonik *et al.*, Phys. Rev. B **82** (2010) 201408(R).
 [9] A. Varlet *et al.*, Phys. Rev. Lett. **113**, 116602 (2014).
 [10] C. Liu *et al.*, Nature Physics **6**, 419 (2010).
 [11] S. Khan *et al.*, Phys. Rev. Lett., **112**, 156401 (2014).
 [12] S. Nandi *et al.*, Phys. Rev. Lett., **104**, 057006 (2010).
 [13] S. Avci *et al.*, Phys. Rev. B, **85**, 184507 (2012).
 [14] N. Ni *et al.*, Phys. Rev. B, **80**, 024511 (2009).
 [15] A. Thaler *et al.*, Phys. Rev. B, **82**, 014534 (2010).
 [16] S. Kasahara *et al.*, Phys. Rev. B, **81**, 184519 (2010).
 [17] C. Liu *et al.*, Phys. Rev. B **84**, 020509(R) (2011).
 [18] N. Xu *et al.*, Phys. Rev. B **88**, 220508(R) (2013).
 [19] Yong *et al.*, Phys. Rev. B **90**, 224508 (2014).
 [20] Y. Wu, *et al.*, Phys. Rev. Lett. **115**, 166602 (2015).
 [21] I. M. Lifshitz, Sov. Phys. JETP **11**, 1130 (1960).
 [22] K. Quader *et al.*, Phys. Rev. B **90**, 144512 (2014).
 [23] H. Ghosh and S. Sen, J. Alloys Compd. **677**, 245 (2016).
 [24] Y. Wang *et al.*, Phys. Rev. Lett. **114**, 097003 (2015).
 [25] M. R. Norman *et al.*, Nature (London) **392**, 157 (1998).
 [26] H.-B. Yang *et al.*, Nature **456**, 77 (2008).
 [27] H.-B. Yang *et al.*, Phys. Rev. Lett. **107**, 047003 (2011).
 [28] D. LeBoeuf *et al.*, Nature **450**, 533 (2007).
 [29] S. Sebastian *et al.*, PNAS **107**, 6175 (2010).
 [30] S. J. Clark *et al.*, Zeitschrift für Kristallographie **220**(5-6), 567 (2005).
 [31] J. Perdew *et al.*, Phys. Rev. Lett. **77**, 3865 (1996).
 [32] D. Kasinathan, *et al.*, New J. Phys. **11**, 025023 (2009).
 [33] S. Sen, H. Ghosh, Phys. Lett. A **379**, 843 (2015).
 [34] S. Sharma *et al.*, Acta. Cryst. B **71**, 61 (2015).
 [35] S. Sen *et al.*, Supercond. Sci. Technol. **27**, 122003 (2014).
 [36] M. Rotter, High-temperature superconductivity in doped BaFe₂As₂, PhD thesis, Ludwig-Maximilians-Universität München, (2010) p. 61.
 [37] A. S. Sefat *et al.*, Phys. Rev. Lett. **101**, 117004 (2008).
 [38] L. Bellaiche *et al.*, Phys. Rev. B, **61**, 7877 (2000).
 [39] M. Rotter *et al.*, Phys. Rev. B **78**, 020503(R) (2008).
 [40] S. Sen and H. Ghosh, J. Alloys Compd. **675**, 416 (2016).
 [41] R. S. Dhaka *et al.*, Phys. Rev. Lett., **110**, 067002 (2013).
 [42] S. Avci, *et al.*, Phys. Rev. B, **88**, 094510 (2013).
 [43] J. M. Allred *et al.*, Phys. Rev. B, **90**, 104513 (2014).
 [44] S. Ideta *et al.*, Phys. Rev. Lett. **110** 107007 (2013).
 [45] A clear case of this may be recognized from the fact that the T_c of (CaFeAs)₁₀Pt_{3.58}As₈ is twice as high as that of (CaFe_{0.95}Pt_{0.05}As)₁₀Pt₃As₈; S. Thirupathaiah *et al.*, Phys. Rev. B. **88**140505 (2013).